

Report on the meteorological conditions in the south-east Pacific area
and large-scale and synoptic forcing during leg 2 of the VOCALS
2008 cruise on the NOAA research vessel R.H.Brown

Thomas Toniazzo*

1 Introduction

The present document presents examples of the relationship between the local conditions and the synoptic-scale meteorology observed during the second half of the VOCALS-REx campaign, and specifically on leg 2 of the VOCALS cruise with the NOAA research vessel R.H.Brown between 9 November and 2 December.

The results and considerations contained herein are still of a preliminary nature and subject to active investigation. Use was made of data from the VOCALS field catalogue (<http://catalog.eol.ucar.edu/vocals/index.html>) and of NCEP/NCAR reanalysis data (Kalnay, E. and Coauthors, 1996: The NCEP/NCAR Reanalysis 40-year Project. Bull. Amer. Meteor. Soc., 77, 437-471). In the Figures below, images are reproduced from those provided by the NOAA/ESRL Physical Sciences Division, Boulder Colorado in their web site <http://www.cdc.noaa.gov/>. We shall refer to this source as NOAA/ESRL in the captions, were relevant.

*NCAS-Climate, Department of Meteorology, University of Reading, RG6 6BB, UK; t.toniazzo@reading.ac.uk

2 State of the south-Pacific subtropical anticyclone and its relation with the large-scale circulation

The large-scale circulation in the south-east Pacific (SEP) is controlled by the sub-tropical anticyclone, characterised by a permanent high sea-level pressure (SLP), a shallow boundary layer capped by thin stratiform cloud and a strong inversion, and subsidence in the free troposphere (Figure 1, top). It represents the radiatively cooling branch of the Pacific Walker-Hadley circulation connected with the semi-permanent areas of cumulus convection over the West Pacific, the Maritime Continent (the archipelago comprising Java, Sumatra, Borneo and New Guinea) and in the east-Pacific inter-tropical convergence zone (ITCZ) north of the Equator (mainly the area of the Gulf of Panama). The pressure difference between the subtropical anticyclone and these areas of active convection determines the strength of the surface circulation in the tropics and hence affects the air-sea fluxes and the thermal and dynamical structure of the lower atmosphere and of the upper ocean.

The anticyclone was deeper and wider than normal during the first half of VOCALS-REx (Figure 1, panel in the middle). At the same time, pressure was lower in the southern mid-latitudes. A similar dipolar pattern is observed also in the upper troposphere (Figure 1, bottom panel). This suggests that the concomitant strengthening of the subtropical anticyclone and of the mid-latitude storm track, and a larger potential for baroclinic wave activity and a larger exchange of momentum between the tropics and the southern extratropics, consistently with the intensified tropical circulation implied by the SLP pattern.

A net transfer of momentum preceding the Oct-Nov anomalies is indicated in Figure 2, showing a reduction of the angular momentum in the tropics in the second half of September, followed by a corresponding increase in mid-latitudes. This may be surmised to be a consequence of increased transport by baroclinic eddies, consistently with the H200 anomaly pattern.

A typical mechanism for the initial development for persistent circulation anomalies in the mid-latitudes is represented by quasi-stationary Rossby wave-trains generated by upper-level divergence from anomalous tropical convection. The upper-level anomalies of the streamfunction (which represents the rotational part of the flow, associated with its adiabatic, inviscid component) for September 2008, shown in Figure 3 (upper panel), have

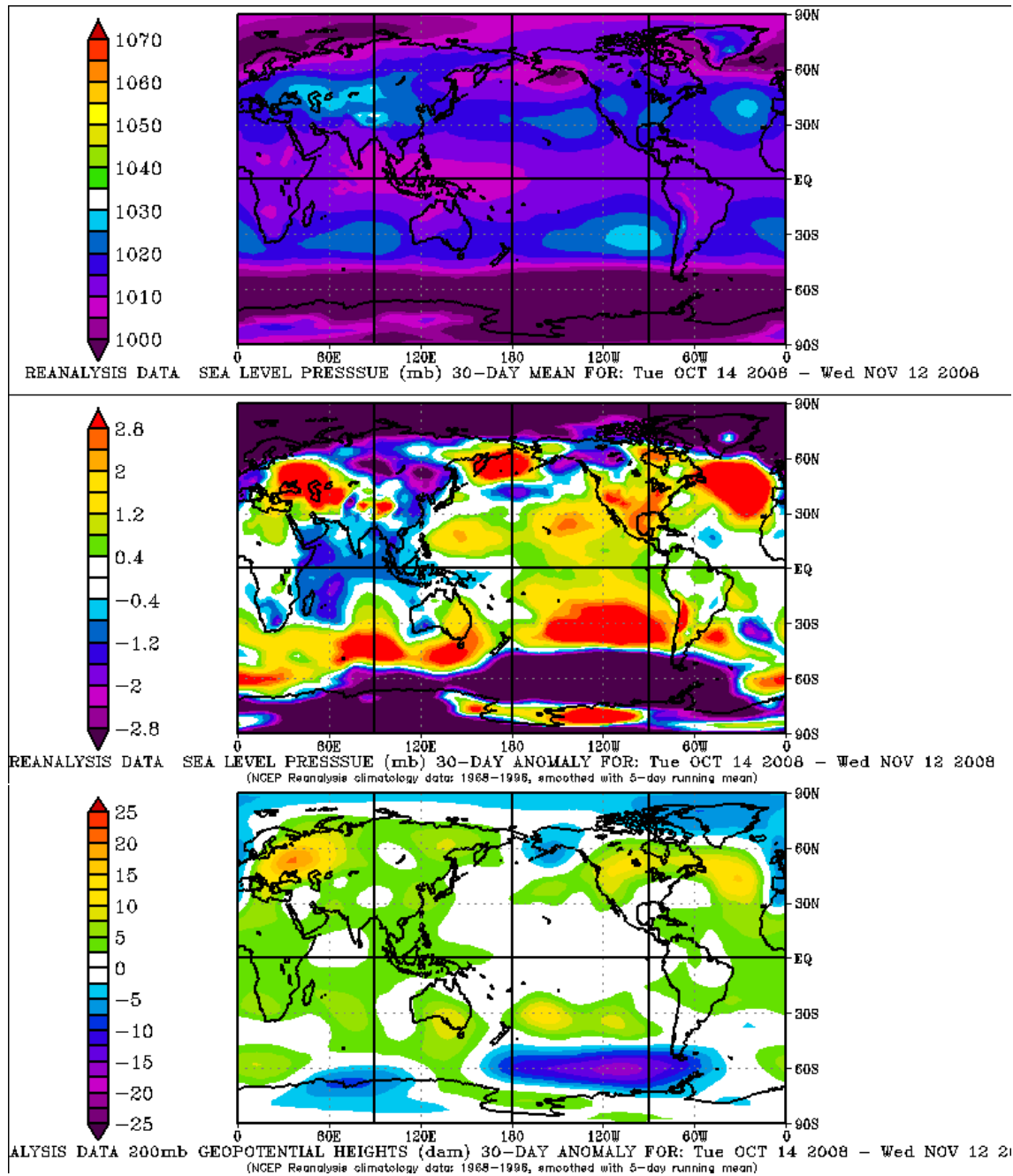


Figure 1: Mean sea-level pressure (panel at the top), and mean anomalies with respect to the climatology (1968-1996) of sea-level pressure (middle panel) and geopotential height at 200 hPa (bottom) for the period between 14 October 2008 and 12 November 2008. Here and in the following the anomalies are defined as differences from the mean monthly climatology over the years 1968-1996. Images from NOAA/ESRL.

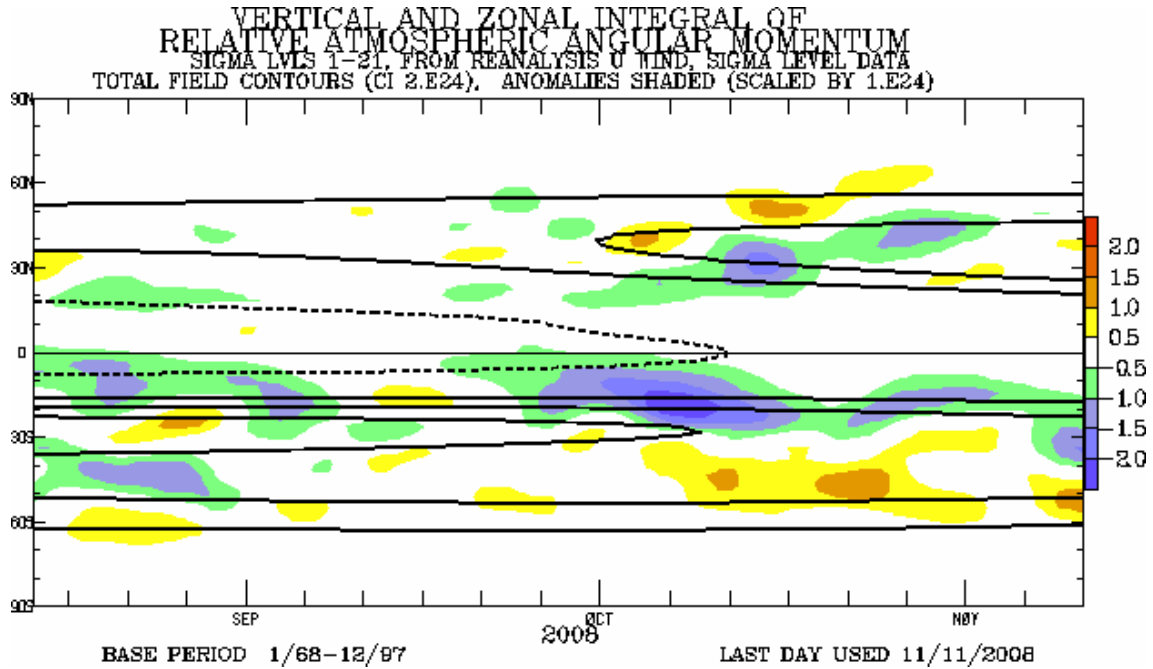


Figure 2: Relative angular momentum of the atmosphere as a function of time (on the abscissae) and latitude (ordinates). The contour interval is 2×10^{24} g cm/s for the total field (line contours) and $\times 10^{24}$ g cm/s for the anomalies (colour coding). Image from NOAA/ESRL.

the appearance of such a wave-train. In geopotential height (not shown), they are barotropic (i.e. they have the same pattern, with the same sign, at all pressure levels), and with a degree of symmetry about the Equator (consistently with the parallel development of zonal momentum anomalies in the northern mid-latitudes, as seen in Figure 2). Together with the streamfunction anomalies, Figure 3 shows the anomalies in the velocity potential, bottom panel), the gradient of which gives the divergent part of the flow, typically associated with diabatic heating and surface friction. The pattern observed implies upper-level divergence over the Maritime Continent region and upper-level convergence over the central and western Pacific, relative to the 1968-1996 climatological mean for September. Areas of upper-level divergence are sources of vorticity which can excite meridionally propagating Rossby waves, and they are associated with ascent typically forced by condensational heating in cumulus convection.

The velocity potential pattern seen in the bottom panel of Figure 3 is qualitatively consistent with a station-

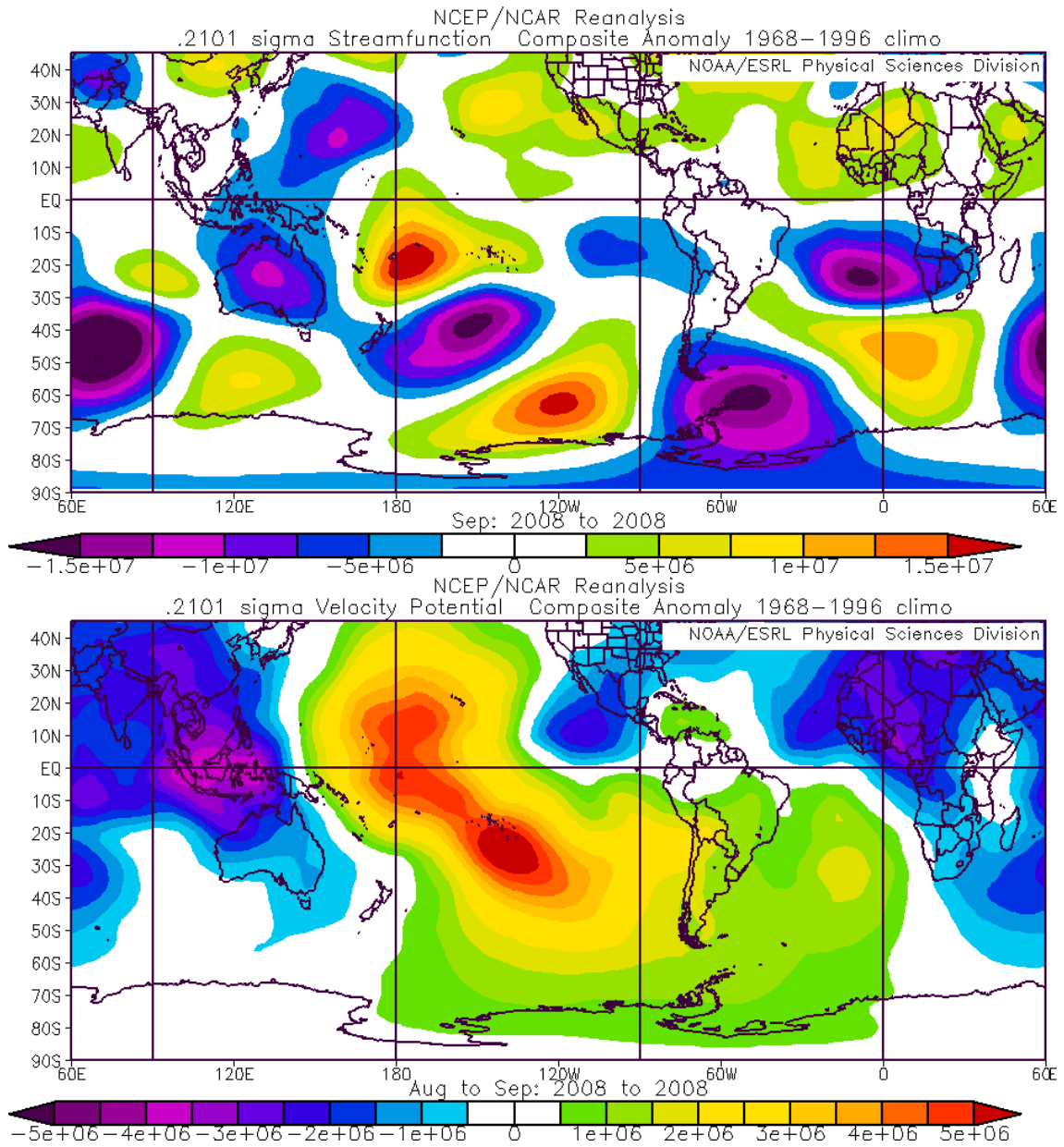


Figure 3: September 2008 anomalies of the streamfunction (panel at the top) and the velocity potential (panel at the bottom) at the level $\sigma = 0.21$ ($\sigma \equiv p/p_*$ where p_* is the pressure at the surface). Images from NOAA/ESRL.

ary Rossby wave-train with a streamfunction similar to that seen in the upper panel of the Figure. Moreover, its geographical location is also qualitatively consistent with convection anomalies during the late phase of the Indian Monsoon season. These are estimated from anomalies in the outgoing longwave radiation (OLR) at the

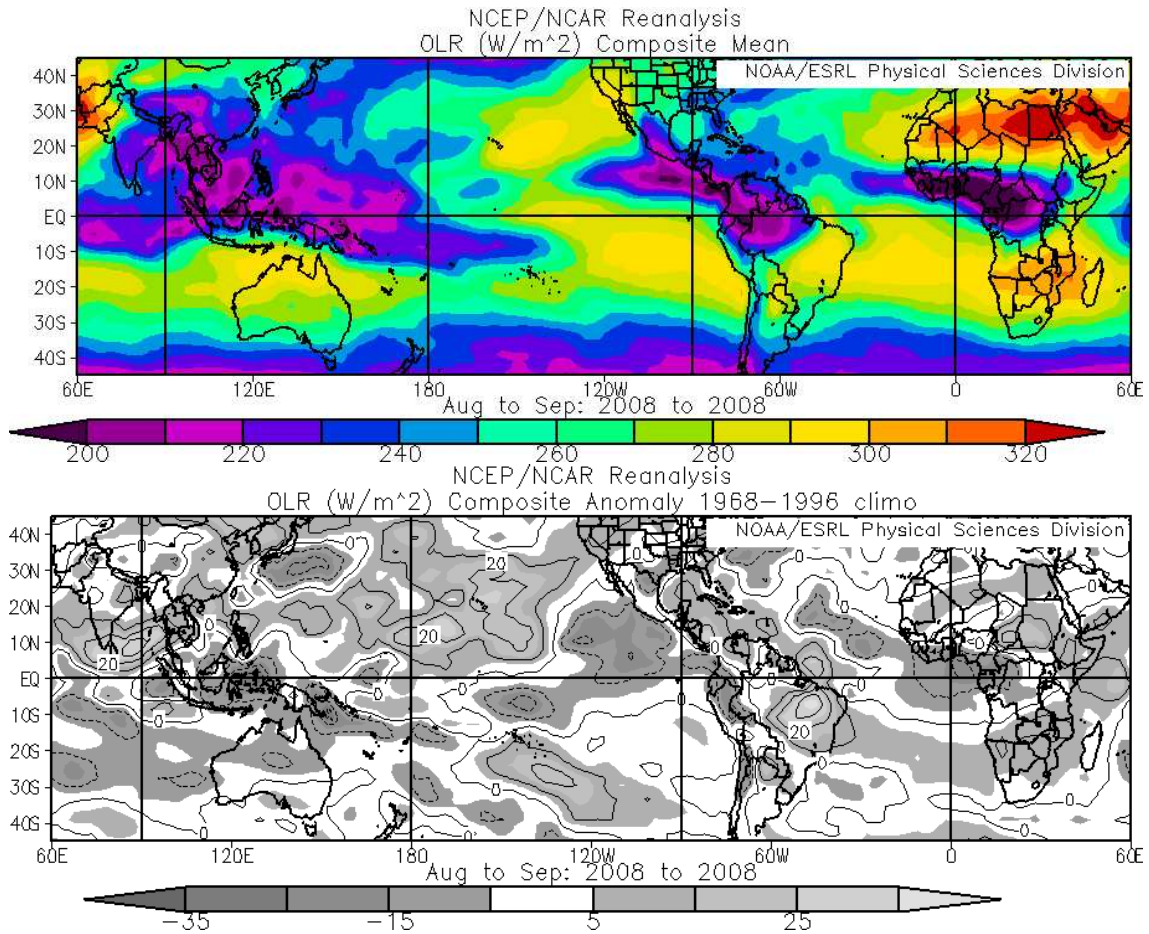


Figure 4: OLR totals (upper panel) and anomalies (lower panel) for the months of August and September 2008. Images from NOAA/ESRL.

top of the atmosphere, shown for August-September 2008 in Figure 4 (upper panel). (The September anomalies are similar, but slightly shifted to the East). The OLR anomalies are most significant in terms of precipitation (and condensational heating) where the cloud-tops are already high and the total OLR (shown in the lower panel of Figure 4 is low. A reduction in long-wave radiation over the Maritime Continent is visible, corresponding with high cloud-tops and greater-than-average precipitation rates.

In summary, we interpret the observations presented here in the following way. The greater-than-average precipitation over the Maritime Continent in the late Monsoon season generated a quasi-stationary, equivalent barotropic Rossby wavetrain in September. In the early southern spring season, the low over the southern

mid-latitude storm-track (seen as a positive streamfunction anomaly in Figure 2) interacted with the baroclinic eddies maintaining the jet stream, resulting in a net transfer of momentum towards the mid-latitudes and giving rise to the barotropic zonal-mean anomaly seen in Figure 1. This results in a stronger-than-average subtropical anticyclone, consistently with the need for greater positive zonal surface stress in the tropics, and the general intensified circulation required to maintain the anomalously strong Hadley/Walker circulation. We maintain that it may be important to bear this mean anomaly in mind when evaluating the mean conditions experienced during VOCALS-REx campaign, at least during its first half.

3 On the influence of the synoptic scale on the Sc cloud field in the VOCALS-REx area

During the course of leg 2 of the VOCALS 2008 cruise with the R.H.Brown it has been observed that the general conditions of the Sc cloud field are to some extent predictable on the basis of the synoptic scale flow alone. Some operational models, such as the UK Met Office Unified Model, show some skill in their forecasts of the cloud cover and of the cloud liquid water if considering changes in their general pattern. However, allowances need to be made for model biases. For example, the UKMO Unified Model tends to overproduce cloud, especially within a few hundred of km from the coast, where it also fails to generate the diurnal clearing.

It has however turned out to be useful to compare the synoptic-scale flow above the cloud top inversion (generally between 850 and 800 hPa), for which reanalysis and forecasts are reliable and consistent between different forecast times and between different models, with the satellite images in the visible band, and reason on the tendencies for the next day. In general terms, there appears to be a significant relationship between lofting implied by the quasi-geostrophic flow in the free troposphere (for example from PV conservation and vorticity advection) and cloud cover, in the sense of decreasing cloud cover with increased lofting. The resulting cloud field appears affected by the combination from such tendencies and the advection with the mean south-south-easterly PBL winds.

In the remainder of this section we give an example of such relationship between synoptic-scale flow and cloud



Figure 5: Photograph taken in the morning of 15 November (near 11UTC) looking north-east from the deck of the R.H.Brown.

field based on the evolution over a day between November 14 and 15, when a coastally-trapped sub-synoptic low formed in the vicinity of the ship (which was downstream of the low, near 19.5S, 76W). The cloud field on 15 November appeared both thin, non-drizzling, and characterised by regular features extending over tens of km (Figure 5). Figure 6 shows a comparison between the Sc cloud cover and the synoptic flow at 500 hPa. On the 14th, cloud-free areas appear in the south-east of the satellite image which correspond with the north-east side of the 500hPa cyclone where quasi-geostrophic lofting can be expected. In the area of quasi-geostrophic subsidence to the north-west the cloud cover persists. Further to the north, the liquid water part (not shown) was high and an region of “open cells” appears north of 20S. The evolution of this cloud field into the following day is broadly consistent with mean PBL-wind advection to the north-west, but the area of clearing moves

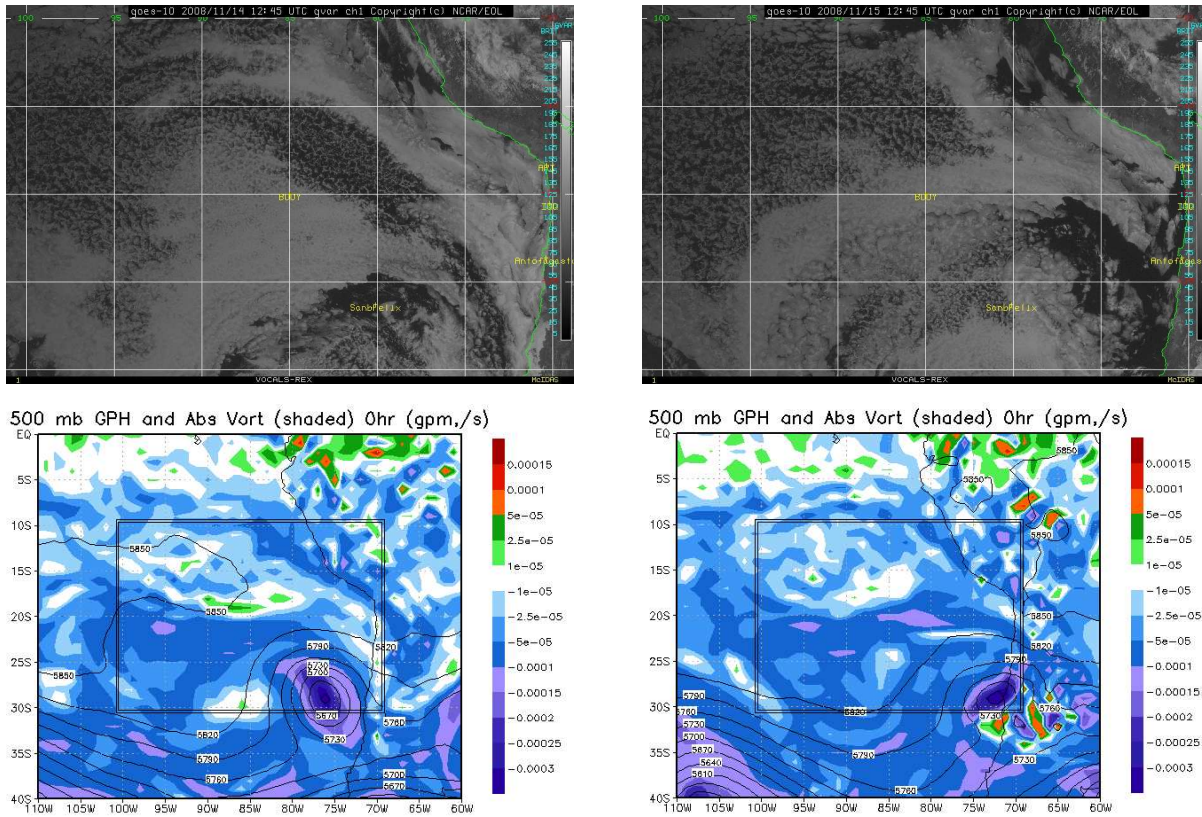


Figure 6: Visible (channel 1) images of the GOES satellite over the VOCALS region (panel at the top) and model reanalysis fields of 500hPa geopotential height (lower panels, contour lines) and absolute vorticity (lower panels, colour coding) for the days of 14 November and 15 November 2008. The validity time of the satellite images is 12.45 UTC, those of the model fields is 12.00 UTC. The rectangles in the model fields show the field-of-view of the satellite images. The reanalysis fields are from the NCEP GFS 40km model. Images from the VOCALS field catalogue.

eastward together with the cyclone aloft, and it intensifies near the coast.

Figure 7 shows the free-tropospheric lofting as represented in the GFS reanalysis. The 800hPa pressure velocity in the late evening between November 14 and 15 (00UTC=21LT is about an hour after sunset) is qualitatively consistent with conservation of potential vorticity (PV) in the geostrophic flow aloft, where increasing absolute vorticity is compensated by vortex stretching. Additionally, the upsidence wave from diurnal heating of the coastal orography is visible near the Peruvian coast. In the morning hours (12UTC=9LT), a northerly

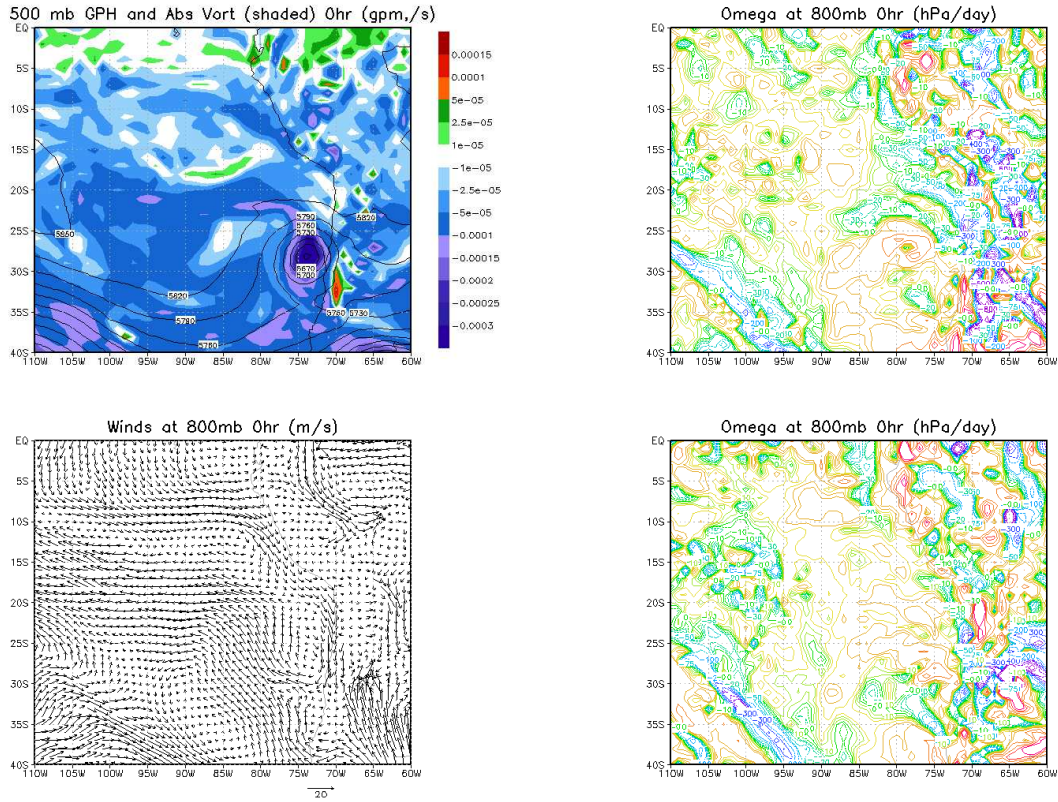


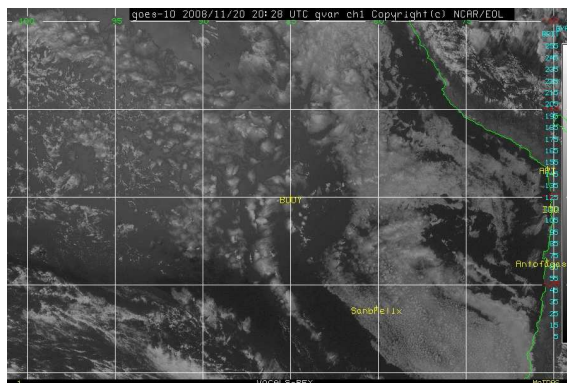
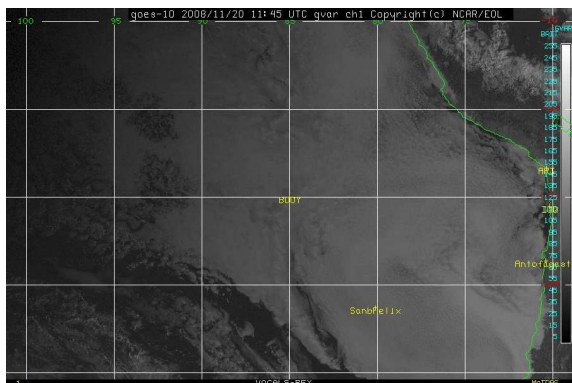
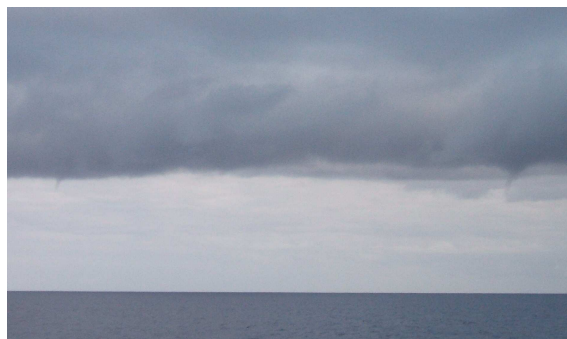
Figure 7: GFS reanalysis model fields valid for 00UTC (panels at the top) and for 12UTC (panels at the bottom) on Nov 15 2008. *Top left*: geopotential height (contour lines) and absolute vorticity (colour coding) at 500 hPa; *Bottom left*: horizontal winds at 800 hPa; *Left-hand side*: pressure velocity at 800hPa. Images from the VOCALS field catalogue.

coastal jet develops. Northerly flow is normally generated by orographic blocking under high stability, but the reversed pressure gradient associated with the CTD (with lower pressure to the south) increases its strength and maintains it through the day. The cyclonic flow around the low pressure system is evident. Both PV conservation and Ekman pumping from surface friction (greater over land than over sea) force atmospheric ascent over the coastal waters, as seen in the last panel on the bottom-right of Figure 7.

Although the details of the cloud field depend on the microphysics and on the history of the air-mass, and cannot be understood from synoptic conditions, the relatively good match between the pressure velocity in the reanalysis fields and the features visible in the satellite and in-situ observations of cloud cover noted above

Figure 8: Cloud observations for November 20 2008.

Right: photographs taken from the deck of the R.H.Brown (19.5S, 84.5W), looking north-east, of funnel clouds at about 8.30LT (11.30UTC). *Below:* GOES visible images of the VOCALS area for November 20 2008, at 8.45LT and at 17.28LT on the left-hand side and on the right-hand side, respectively. Satellite images from the VOCALS field catalogue.



are remarkable in that the GFS model produces nearly no cloud whatsoever. This implies not only that cloud respond to synoptic forcing at leading order, but also that, over short time leads, the synoptic-scale flow is not significantly altered by the presence of cloud. This might help explaining why some forecast models, such as the UKMO Unified Model and the ECMWF model, can produce realistic-looking cloud fields and relatively accurate forecasts even with their simple representation of cloud microphysical processes.

4 The synoptic-scale conditions between November 20-30

The second half of leg 2 of the R.H.Brown cruise was characterised by frequent high liquid-water path, relatively thick and precipitating cloud early in the day, and clearing in the afternoon. The morning of November 20, at the beginning of this period, was particularly remarkable in that the cloud layer (where RH exceeds 95% in the

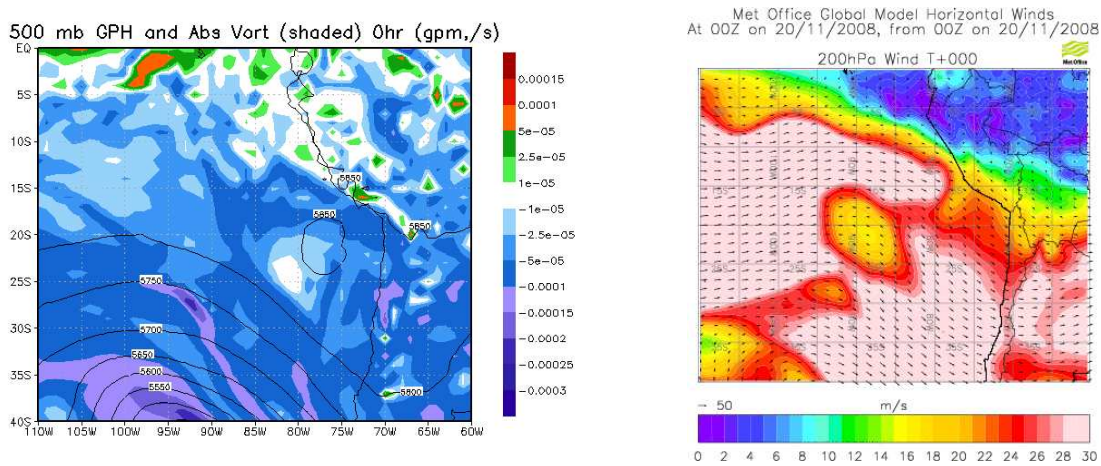


Figure 9: Reanalysis fields of 500hPa geopotential height and absolute vorticity (left; contour lines for height and colour-coding for vorticity), and for 200hPa winds (right) on November 20, 2008. Images from the VOCALS field catalogue.

radiosonde readings) appeared to be well over 1 km thick, precipitation was widespread (with raindrops reaching the ship's deck) and funnel clouds developing off a visibly subsiding cloud protuberance from a precipitating cloud cluster were observed (Figure 4, panel on the top). The cloud cluster was part of a linear formation of thicker cloud visible from the satellite (panel on the bottom-left in Figure 4), extending from the south of the ship. In the afternoon, the sky cleared almost completely (panel on the bottom-right in Figure 4).

The circulation at 500hPa and 200hPa on that day shows poleward flow aloft of the ship's location and general VOCALS area (Figure 9). This implies ascent from vortex stretching in PV-conserving motion, weakening the radiatively-driven subsidence. Additionally, in the following days the formation of a moist layer ($RH \sim 30\%$) in the upper troposphere ($p \sim 250$ hPa) was observed in the radiosonde profiles. This further slows the climatological subsidence by reducing long-wave cooling.

The 200hPa trough in the South Pacific, west of the VOCALS area, is part of a large-scale anomaly consistent with a planetary wave pattern with zonal wave-numbers 4 and 5 (Figure 10). The origin of planetary wave-trains of this kind, outside the Indian Monsoon season, is often due to convective activity in the Indian Ocean associated with the Madden-Julian Oscillation. That it may be the cause also for this case is confirmed by the observed OLR anomalies in the preceding week, shown in Figure 11 (panel on the left-hand side). A time-

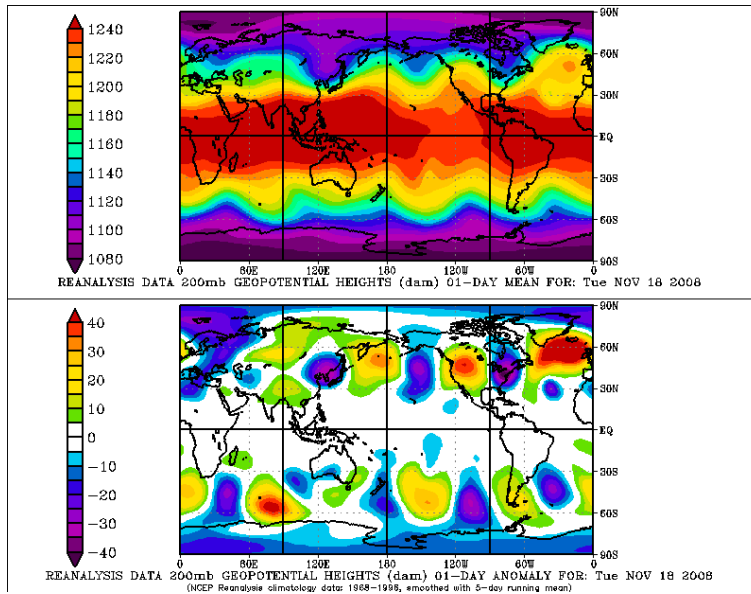


Figure 10: Geopotential height (top) and height anomalies (bottom) at 200hPa for November 18, 2008. Image from NOAA/ESRL.

longitude diagram of total OLR with the equatorial band (7.5M-7.5S) (Figure 11, panel on the right-hand side) indicates that the MJO was very active during October and November 2008. In particular, the MJO was in its positive phase (with increased convection over the Indian Ocean and the Maritime Continent) starting from November 10.

As the typical period of the oscillation is between 30 and 60 days, the circulation anomalies are also relatively long-lived, and can persist for over 10 days in the extratropics even if carried by a wave-train with wave-number different from the stationary one. This gives good predicatbility of these global teleconnection with forecast models. The persistence of the poleward flow aloft within the VOCALS area was noted on November 20 and on that basis it was predicted that morning drizzle and afternoon clearing would continue for the next 10 days. The forecasts were qualitatively accurate in that poleward flow indeed persisted, as shown in Figure 12. Figure 13 shows the 500hPa circulation for November 22-28, with baroclinic eddies generated in the displaced jet-stream at the southern edge of the VOCALS region. The trough eventually dissipated on November 30.

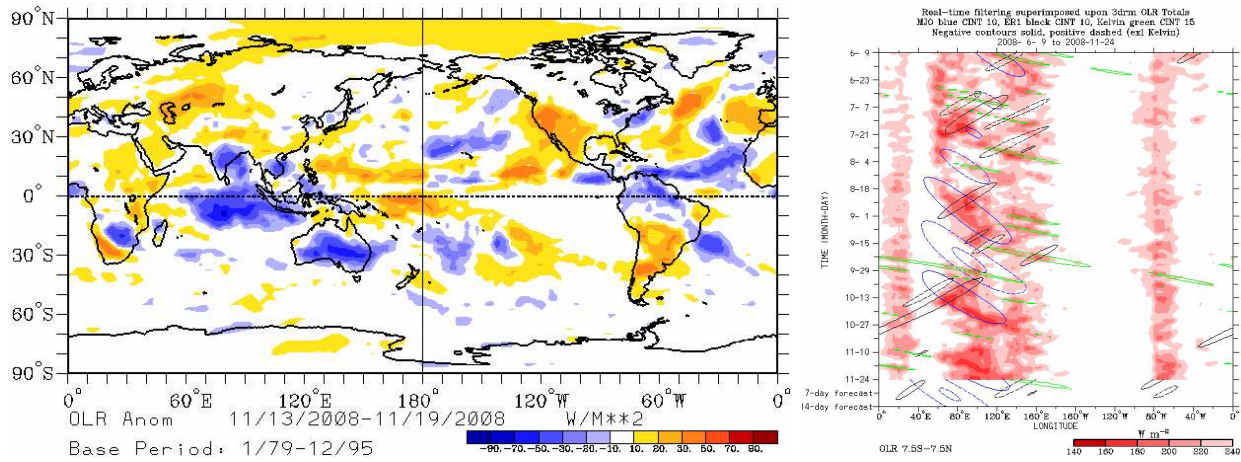


Figure 11: *Left*: OLR anomalies for the period 13-18 November 2008. *Right*: total OLR between 7.5S and 7.5N as a function of longitude (on the x-axis) and time (on the y-axis, increasing downward). Blue circles identify MJO modes of variability. Images from NOAA/ESRL.

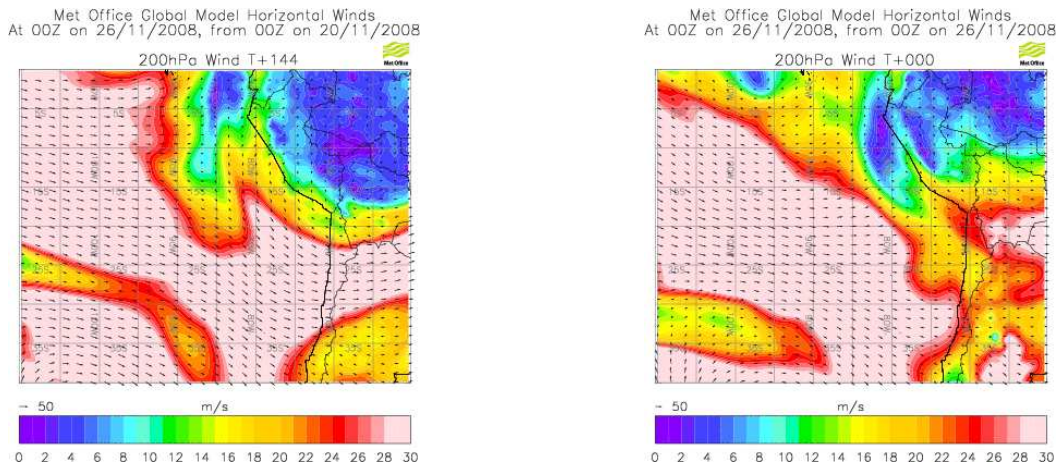


Figure 12: Forecast fields of November 20 for the 200hPa winds at 6 days lead time (panel on the left-hand side), and at reanalysis on November 26, from the UKMO Unified Model. Poleward flow aloft in the VOCALS area is present in both fields. Images from the VOCALS field catalogue.

5 Conclusion

The meteorology of the VOCALS region in the South-East Pacific is affected by the large-scale circulation both in the tropics and in the midlatitudes. On the basis of the observations made during the VOCALS-

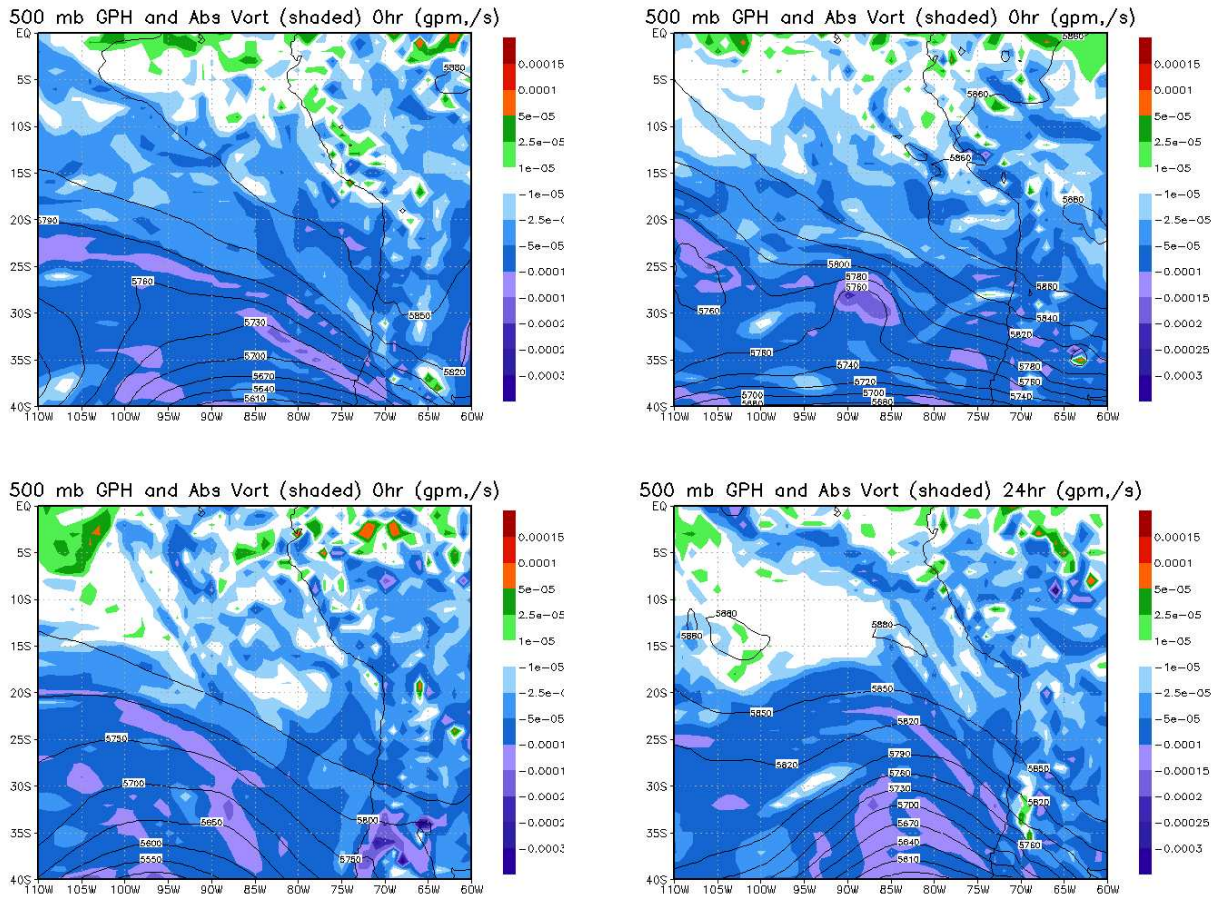


Figure 13: Reanalysis fields of 500hPa geopotential height and absolute vorticity for November 22-28, from the NCEP GFS model. Validity times are 00UTC for November 22, 24, 26, and 28 from top-left to bottom right. Images from the VOCALS field catalogue.

REx campaign, it is suggested here that upper-level advection of moisture and free-tropospheric lofting have a significant effect on the Sc cloud cover during spring, by affecting the rate of tropospheric subsidence which maintains the PBL-capping inversion. Three case studies are sketched in this draft report that suggest that anomalies can be maintained over time-scales from a few days to months. A particular role appears to be played by convection in the area of the eastern Indian Ocean and the West Pacific that can be associated with variability in the south-west Monsoon and with MJO activity.